JUSTC

Article

http://justc.ustc.edu.cn

Received: December 17, 2023; Accepted: May 06, 2024

Evolution of the volume expansion of SiO/C composite electrodes in lithium-ion batteries during aging cycles

Haosong Yang, Kai Sun, Xueyan Li, Peng Tan ✉, and Lili Gong ✉

Department of Thermal Science and Energy Engineering, University of Science and Technology of China, Hefei 230026, China

✉Correspondence: Peng Tan, E-mail: pengtan@ustc.edu.cn; Lili Gong, E-mail: liligong@ustc.edu.cn

Graphical abstract

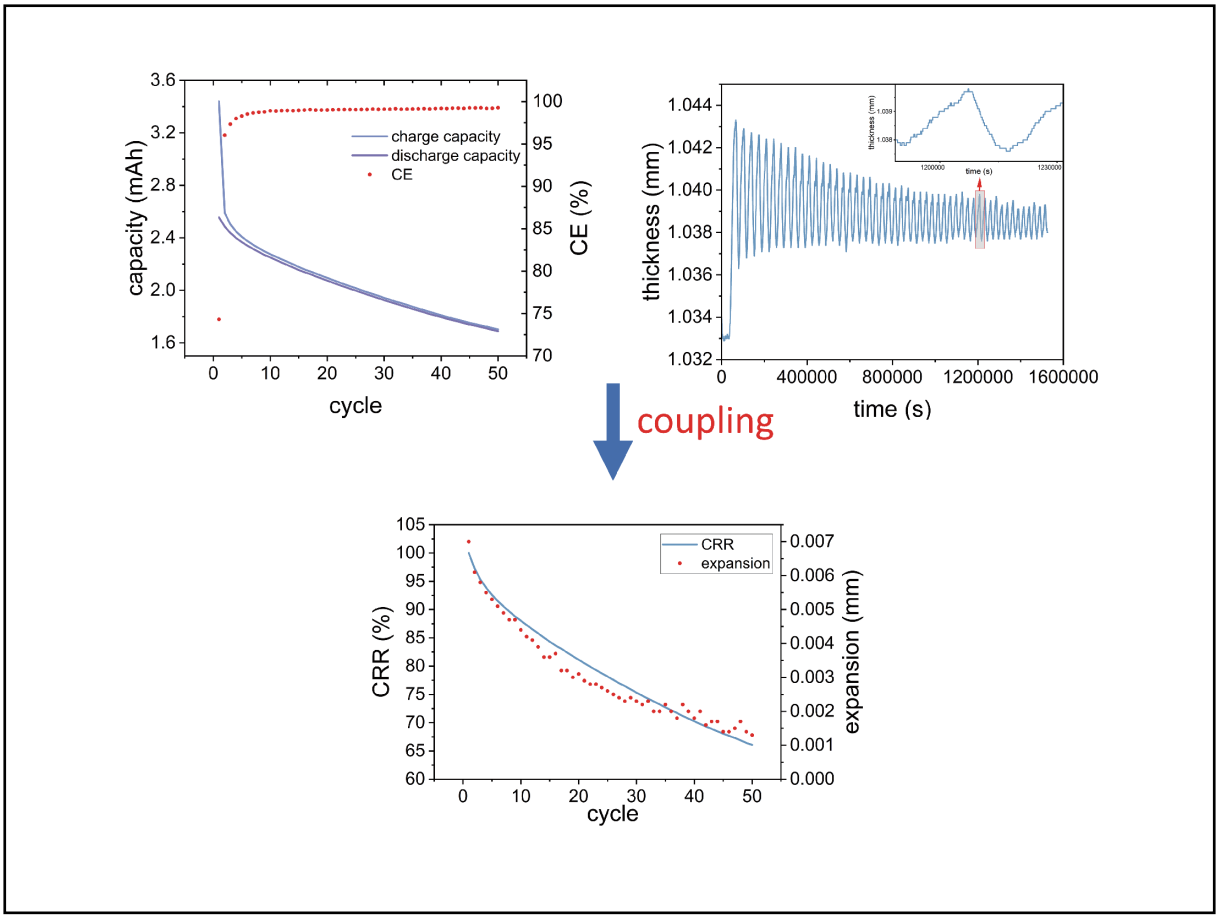

Coupling relationship between the attenuation of battery capacity and the reduction in thickness variation.

Public summary

- We observed a linear relationship between changes in battery thickness and capacity retention ratio.
- The mechanism of external stress on battery performance was analyzed by electrochemical experiments and SEM images.
- These results can be used to improve the performance and prolong the life of lithium-ion batteries.

Citation: Yang H S, Sun K, Li X Y, et al. Evolution of the volume expansion of SiO/C composite electrodes in lithium-ion batteries during aging cycles. *JUSTC*, **2025**, 55(2): 0203. CSTR: 32290.14.JUSTC-2023-0166. DOI: 10.52396/JUSTC-2023-0166

JUSTC

Article

http://justc.ustc.edu.cn

Received: December 17, 2023; Accepted: May 06, 2024

Evolution of the volume expansion of SiO/C composite electrodes in lithium-ion batteries during aging cycles

Haosong Yang, Kai Sun, Xueyan Li, Peng Tan ✉, and Lili Gong ✉

Department of Thermal Science and Energy Engineering, University of Science and Technology of China, Hefei 230026, China

✉Correspondence: Peng Tan, E-mail: pengtan@ustc.edu.cn; Lili Gong, E-mail: liligong@ustc.edu.cn

Cite This: *JUSTC*, **2025**, 55(2): 0203 (7pp)

Read Online

Abstract: As a negative electrode material for lithium-ion batteries, silicon monoxide (SiO) suffers from dramatic volume changes during cycling, causing excessive stress within the electrode and resulting in electrode deformation and fragmentation. This ultimately leads to a decrease in cell capacity. The trends of volume expansion and capacity change of the SiO/graphite (SiO/C) composite electrode during cycling were investigated via in situ expansion monitoring. First, a series of expansion test schemes were designed, and the linear relationship between negative electrode expansion and cell capacity degradation was quantitatively analyzed. Then, the effects of different initial pressures on the long-term cycling performance of the cell were evaluated. Finally, the mechanism of their effects was analyzed by scanning electron microscope. The results show that after 50 cycles, the cell capacity decreases from 2.556 mAh to 1.689 mAh, with a capacity retention ratio (CRR) of only 66.08%. A linear relationship between the capacity retention ratio and thickness expansion was found. Electrochemical measurements and scanning electron microscope images demonstrate that intense stress inhibits the lithiation of the negative electrode and that the electrode is more susceptible to irreversible damage during cycling. Overall, these results reveal the relationship between the cycling performance of SiO and the internal pressure of the electrode from a macroscopic point of view, which provides some reference for the application of SiO/C composite electrodes in lithium-ion batteries.

Keywords: lithium-ion batteries; in situ expansion measurement; initial stress; cycle life; SiO/C composite electrode

CLC number: TM912 **Document code:** A

1 Introduction

With the growing concern for environmental issues, there is a rising demand for the development of new energy and energy storage systems[1–3]. Among many battery systems, lithium-ion batteries (LiBs) are particularly noteworthy because of their high energy density, low self-discharge rate, long cycle life, and excellent portability[4–7]. Graphite is the most commonly used anode material for lithium-ion batteries, but its utilized capacity is close to its theoretical capacity of 372 mAh/g[8], necessitating further development of high-capacity anode materials. The highly anticipated silicon (Si) anode, which stores lithium by forming an alloy, exhibits more than ten times greater theoretical capacity ($Li_{4.4}Si$, 4200 mAh/g)[9,10] than does graphite; however, it has a drastic volume expansion (~300%) during lithiation[11,12] (compared with ~12% graphite[13]). Such a drastic volume change leads to particle pulverization, electrical isolation, and unstable ever-thickening of the solid-electrolyte-interphase (SEI), which results in unacceptable cycle performance[14–16]. In contrast, silicon monoxide (SiO) has a theoretical capacity of at least 1965 mAh/g and a lower volume expansion (~160%)[17,18] and is considered a feasible candidate. However, the capacity of SiO electrodes decreases to less than 80% after 25 cycles[19], and their cycle stability is still not enough to act as a negative electrode alone[20].

Currently, SiO/graphite (SiO/C) composite anodes are often used as a compromise[21]. Similar to Si, the aging mechanism is attributed to the expansion of SiO, leading to particle pulverization, electrode contact failure, and unstable ever-thickening SEI[22,23], and the generation of internal pressure is a key factor in cell capacity reduction and eventual failure[24]. When investigating the expansion and generation of internal pressure in cells, the contribution of cathode materials to the expansion is often neglected, since the volume change during lithiation is only 1.5% of the volume change in SiO (~2.4% for $LiNi_{1/3}Mn_{1/3}Co_{1/3}O_2$ positive electrode materials)[25,26]. Typically, the pressure received by the SiO particles is the superposition of the stress generated by the expansion of the particles and the externally applied stress, which implies that the externally applied initial stress also affects the cell performance[27–29]. Previous research has shown that high levels of stress, similar to low temperature[30], can impact the Li storage behavior of active particles and encourage Li planting[31], and the resulting risks should be assessed[25]. In addition to the electrodes, other parts of the cell are also affected by pressure, such as the diaphragm, whose ion transport is also limited under high pressure[32].

Considering the working conditions of commercial lithium batteries, researchers usually use pouch batteries as the

CSTR: 32290.14.JUSTC-2023-0166
DOI: 10.52396/JUSTC-2023-0166
JUSTC, **2025**, 55(2): 0203

objects of pressure studies[33]. However, there are gaps between the stacked electrodes and the separators in pouch cells, and these gaps can greatly buffer out the stresses due to changes in the electrode volume, leading to a misinterpretation of the expansion characteristics of the cell and the impact of external stresses on cell performance[34,35]. To better clarify the effect of external stresses on electrode behavior, single-layer electrodes and in situ measurement devices are essential. A complete description of the stress changes in the SiO negative electrode over five cycles is presented in the work of Zhang et al[36]. Nevertheless, a description of the electrode stress or volume changes on longer time scales is still lacking.

In this work, the volume change of the electrodes during fifty cycles is completely portrayed, and the effect of external stress on the cycling performance of the material is quantitatively analyzed. First, an in situ dilatometer combined with a charge and discharge tester was used to measure the thickness change and cycling performance, and a strong linear relationship between the capacity retention ratio (CRR) of the cells and the volume changes was revealed. Subsequently, two sets of coin cells were subjected to different initial pressures and cycled for fifty cycles to investigate the effect of external stress on cell performance. Finally, the batteries were disassembled after cycling, and images of the negative electrodes were taken by scanning electron microscope (SEM) to observe the changes in the surface morphology of the electrodes. By comparing the SEM images of the electrodes before and after cycling and under different pressures, the effect of external stress on the cycling performance of the cell was further investigated.

2 Materials and methods

2.1 Material and cell composition

The positive electrode used in the study was made of $LiNi_{0.88}Mn_{0.05}Co_{0.07}O_2$, conductive additive (LiTX300 carbon black/carbon nanotubes), and (PVDF) binder (weight ratio: 97.3∶1.5∶1.2). The anode is composed of SiO, graphite, super P/single-walled carbon nanotubes (SP/SWCNTs), and poly acrylic acid–styrene butadiene rubber (PAA–SBR) with the weight ratio of 18.5∶74∶2∶5.5. The electrolyte is a commercial lithium electrolyte supplied by Candrd. To reduce the influence of electrolyte consumption on the experimental results during cycling, 100 μL of electrolyte was added to the assembly of each cell.

2.2 Test instruments and methods

To eliminate the influence of parts of the button cell other than the electrodes and separator on the stress and expansion measurements, a special fixture is used to measure the expansion of the electrodes. As shown in Fig. 1a, the whole fixture is composed of a thickness sensor, a force spring, a top indenter, and a bottom indenter. During assembly, the positive electrode, separator, and negative electrode are placed in sequence, and the upper pressure head is tightened after the electrode liquid is injected. The force spring in the fixture can exert approximately 5 kg of force on the electrode. The thick sensor on the top detects a tiny displacement of the indenter on the fixture during the cell cycle. The high-precision thickness measurement system can achieve a thickness measurement resolution of 0.1 μm and an accuracy of ±1 μm. The charge and discharge cycle of the cell is realized through the cell tester. During the assembly process, the diameters of the negative electrode and positive electrode were 16 mm and 14 mm, respectively. The capacity ratio of the negative and positive electrodes (N/P) is set to be greater than 1 to avoid the effect of Li plating on the experimental results due to the misalignment of the pole piece.

The CR2032 button cell used in the experiments was assembled in a glove box (Etelux, Laboratory 2000) in the order shown in Fig.1b, where the structures shown are, from top to bottom, the positive case, spring, spacer, positive electrode, polypropylene (Celgard 2500) separator, negative electrode, and negative case. To conduct experiments with different initial stresses, two spacers with a thickness of 0.5 mm are placed in reference cells, and three spacers are placed in test cells to achieve different external stresses at the beginning of the cycle. The cycle steps used in the two experiments are shown in Table 1.

2.3 Characterization method

For the cells in the experiments with different initial stresses, after 50 cycles, the cells are disassembled, and the surface morphology of the anode is observed via a SEM (Phenom Scientific) operating at 10 kV. A new electrode from the same batch was photographed and used as a reference for changes in electrode morphology.

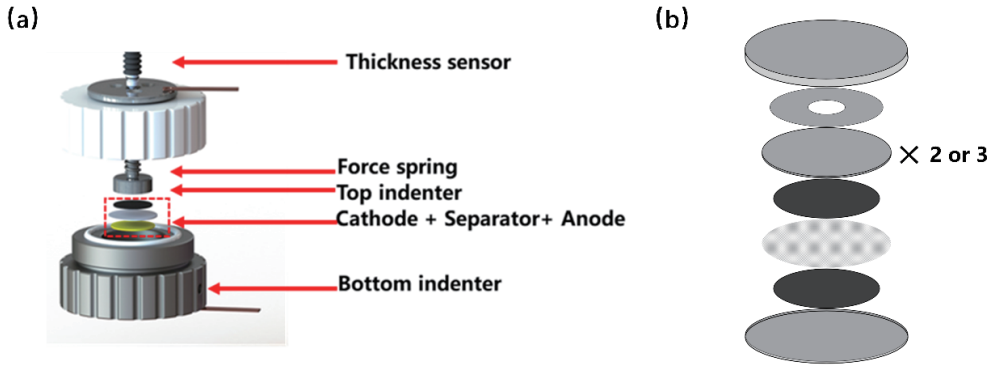

Fig. 1. Schematic diagram of the test fixture. (a) Expansion test fixture. (b) Button cell.

CSTR: 32290.14.JUSTC-2023-0166
DOI: 10.52396/JUSTC-2023-0166
JUSTC, **2025**, 55(2): 0203

Table 1. Experimental work step data.

Serial number	Step	Current (mA)	Stop condition
1	Rest for 24 h		
2	Constant current charge	3	Cutoff voltage of 4.25 V
3	Rest for 10 min		
4	Constant current discharge	3	Cutoff voltage of 2.5 V
5	Rest for 10 min		
6	Cycle 2–5		50 times
7	End		

3 Results and discussion

3.1 In situ expansion test

Owing to the reduction in the size of the positive electrode, the capacity of the in situ expansion experiment cell is limited by the positive electrode capacity, so the total capacity of the cell is slightly smaller than that of the cell in the subsequent external stress experiment. Fig. 2a shows that the cycle process of the cell in the fixture is relatively stable, and the cell maintains a high Coulombic efficiency (CE) of more than 95% in all the cycles except the first one, which indicates that the cell has almost no side reactions during charging and discharging. The main reason of the low CE in the first cycle is that the formation of the SEI film consumes lithium ions, which could be coped with pre-lithiation[37,38].

In conjunction with Fig. 2b, it is worth noting that the cell in this experiment had a lower cycle life than did the commercial cell. As the cycle progresses, the discharge platform of the cell decreases continuously. As shown in Fig. 2b, after completing fifty cycles, the low voltage of the cell discharge platform increased from 3.1 V to approximately 3.4 V, and the capacity decreased from 2.556 mAh to 1.689 mAh, which indicates that the electrode structure of the cell experienced irreversible damage. For lithium-ion batteries with silicon-carbon anodes, the performance first increases and then decreases with increasing applied stress, and the optimal performance point occurs near 0.02 MPa[39]. According to the estimation, the initial stress on the cell in this fixture exceeds 0.1 MPa; obviously, the cycle performance of the cell is greatly damaged under this stress.

Fig. 2c shows the thickness curve of the cell during the fifty cycles. It is easy to correlate thickness changes with the number of charge–discharge cycles. As the cycle progresses, the volume of the electrode after discharge increases continuously compared with that in the previous cycle, which indicates irreversible changes in the electrode structure after the cycle, such as the formation and thickening of the SEI and Li planting. Correspondingly, the volume of the cell after charging continues to shrink compared with that in the previous cycle.

By subtracting the thickness after the end of discharge from the thickness after the end of charge of each cycle of the cell, the thickness change in each cycle of the cell is obtained, the CRR of the cell is drawn in the same graph, and Fig. 2d is obtained. Since the capacity decay of the cell is accompanied by a significant reduction in the expansion of the volume during charging, it can be hypothesized that the capacity decay of the cell at this point mainly comes from the capacity loss of the SiO particles. To further explore the relationship between the

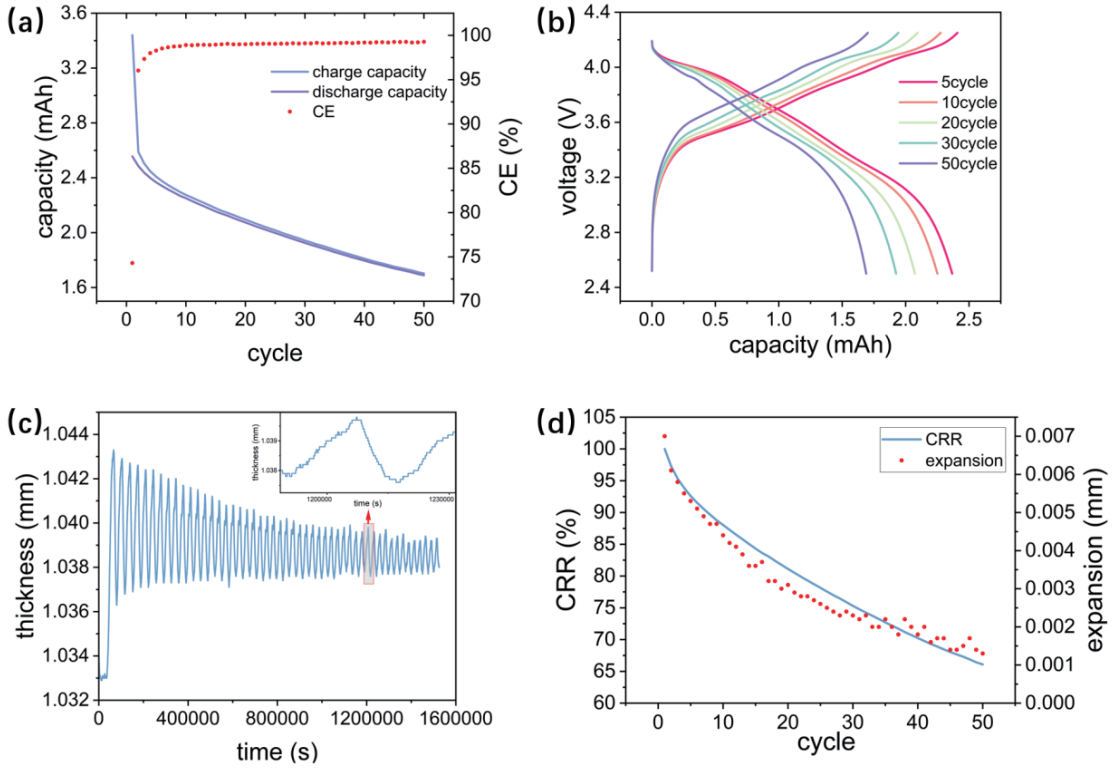

Fig. 2. Cycling performance. (a) Capacity retention and CE curves; (b) charge and discharge curves; (c) thickness variation curve; (d) CRR and expansion curves.

CSTR: 32290.14.JUSTC-2023-0166
DOI: 10.52396/JUSTC-2023-0166
JUSTC, **2025**, 55(2): 0203

two sets of data, a correlation analysis was conducted, and the Pearson's R value between the two sets of data was 0.981, which means that the two sets of data are almost linearly correlated. This means that the aging of a cell can be directly determined by monitoring its stress or volume expansion.

3.2 External stress test

After fifty cycles of charging and discharging of the two groups of batteries, their cyclic charging and discharging curves and capacity change curves are obtained, as shown in Fig. 3. Fig. 3a and b show the charge and discharge curves of the reference cell and the test cell at the 5th, 10th, 20th, 30th, and 50th cycles, respectively. The charge and discharge platforms of the two are relatively similar, but the reference cell can still show perfect consistency in the first half of the charging stage and discharge stage with the progress of the cycle, and the slope of the discharge platform is slightly reduced in the second half of the discharge only from 30 laps. According to the data in Fig. 3c, the reference cell can maintain more than 90% CRR throughout a 50-turn cycle. For the test cell, the charge–discharge curve fluctuates from the 20th cycle, and the stability of the discharge platform during the cycle is lower than that of the reference cell. Combined with the data in Fig. 3d, the CRR of the test cell once dropped to 80% during the cycle, and the CE fluctuation was also lower than that of the reference cell. This indicates that as the external initial stress increases, the stresses generated by the cell during the cycles will act on the electrodes themselves in coupling with the initial stresses, leading to an increase in electrode instability and promoting the occurrence of side reactions. At the cell level, this is reflected in the significant acceleration of cell capacity attenuation, resulting in a lower cycle life. Additionally, there are more pronounced CE fluctuations, indicating increased side reactions during charging and discharging.

It is not sufficient to describe the charge–discharge cycle behavior of the cell through only the cycle curve and other data obtained from electrochemical measurements. To observe the changes in the morphology characteristics of the electrode materials inside the cell during cycling, a fully charged cell, an empty cell of the reference cell, and an empty test cell were disassembled separately at the end of the cycles. A new electrode will be subjected to SEM characterization along with the electrodes obtained from these dismantled batteries to observe the changes in their morphology. The SEM images are shown in Fig. 4, where a–d are electrode surface topography images and e–g are electrode microstructure images.

Fig. 4a shows that the electrode material presents obvious particle accumulation in the initial state. The dark part of the figure is graphite, and the bright part is SiO. Fig. 4b shows that expansion occurs inside the electrode in the fully charged state, but the surface of the electrode forms a pressurized plane due to space constraints, and cracks are generated at the same time. Combined with Fig. 4e–g, it can be seen that after charging, due to the embedding of lithium ions the anode material expands to a spherical shape, and the voids inside the electrodes are filled, increasing the saturation of the whole material. After complete discharge, the particles of the electrode material underwent significant shrinkage and formed

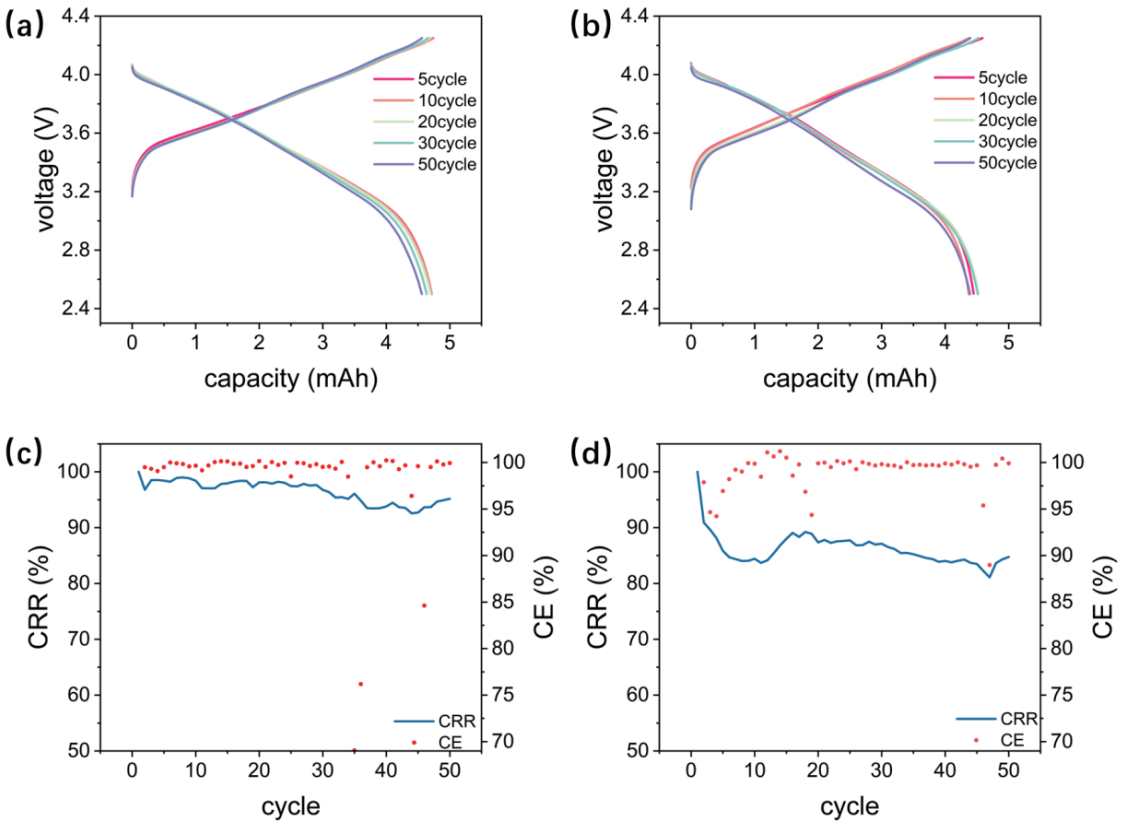

Fig. 3. Charge and discharge curves under different initial pressures: (a) Reference cell, (b) test cell. CRR and CE curves for the (c) reference cell and (d) test cell.

CSTR: 32290.14.JUSTC-2023-0166
DOI: 10.52396/JUSTC-2023-0166
JUSTC, **2025**, 55(2): 0203

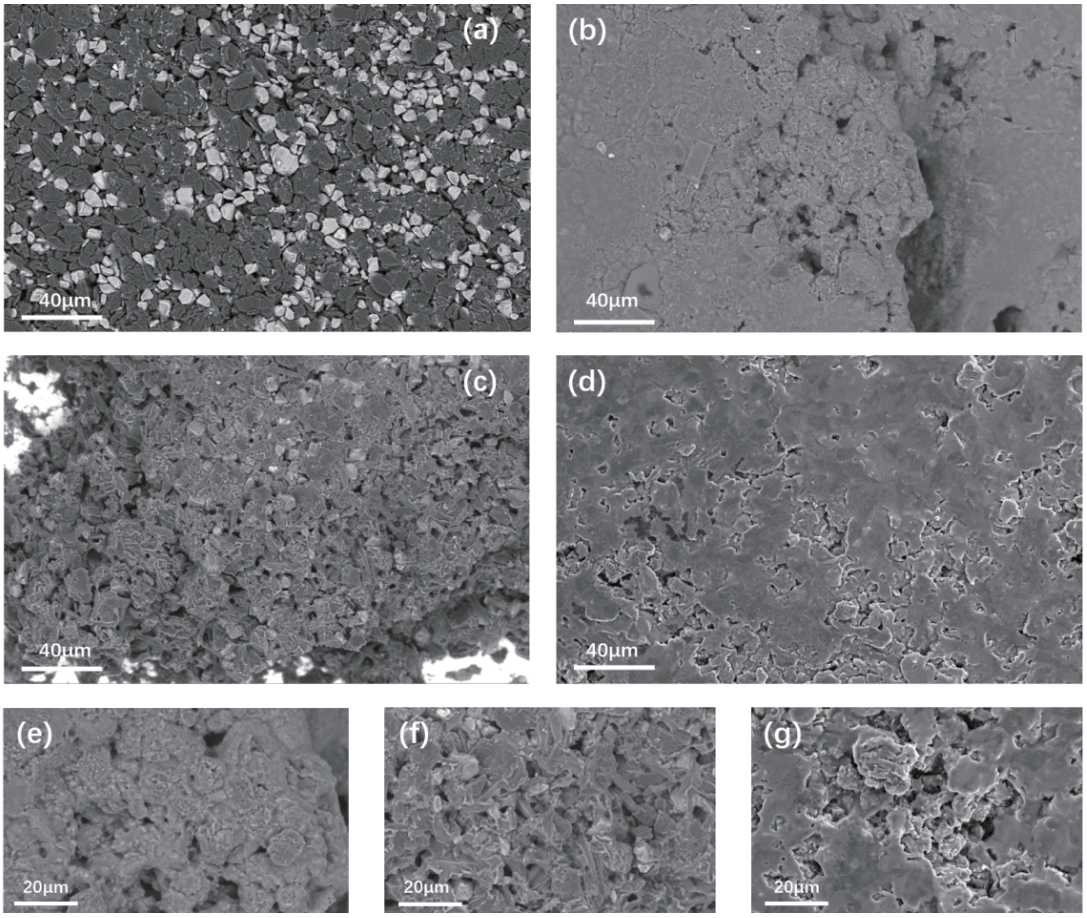

Fig. 4. SEM image of the electrode: (a) New electrode, (b) fully charged electrode, (c) fully discharged test electrode, (d) fully discharged reference electrode. (e) Magnified image of the electrode in (b). (f) Magnified image of the electrode in (c). (g) Magnified image of the electrode in (d).

defects on the surface, but there was still a significant increase in the volume of the active substance particles compared to the new electrode. For the reference electrode, a flat surface can still be seen in the fully discharged state, as shown in Fig. 4d. However, as the active material shrinks in size with the addition of lithium-ions, many defects can be seen on the flat surface. For the test electrodes, the fragmentation of the electrodes deepened and the planar surfaces still existed, as shown in Fig. 4c. At this time, the unreacted active material particles are clearer, and magnified observation shows that some of the particles are in a semi-amorphous state, indicating that these particles can't continue to react in the lithiation due to the presence of external pressure.

4 Conclusions

In the present study, an in situ dilatometer was used to scrutinize the transformation of cell thickness over the charge–discharge cycle, and a linear relationship was found between the decrease in cell capacity and the decrease in expansion. After 50 cycles, the cell's CRR decreased to 66.09%, and the charging-induced thickness expansion decreased from 0.007 mm in the initial cycle to 0.0013 mm. Correlation analysis was performed between the CRR and expansion of the cell, and a Pearson's R of 0.981 was obtained, indicating a strong linear correlation. This suggests that the main contribution to the reduction in cell capacity comes from the materials inside the battery that expand violently upon lithiation. Combined with the volume expansion of SiO and C upon lithiation, the capacity decay of the cell is mainly due to the capacity decay of SiO. Different initial stresses were then applied with varying gasket thicknesses to investigate their impact on cell performance. After the fifth cycle of activation, the reference cell's capacity was found to be 4.74 mAh, whereas that of the test cell was only 4.44 mAh. As the cycle progressed, the reference cell's capacity retention rate remained over 92.5%. In contrast, the capacity retention rate of the test cell decreased to less than 90% after the third cycle, with the capacity retention rate remaining at only 81.09% during the 47th cycle. The SEM images indicate that high pressure inhibits the storage capacity of lithium ions in the negative electrode material of the cell. Furthermore, after cycling, the electrode surface will fracture, leading to a reduced initial capacity and lifespan of the cell.

Moreover, there is still much to be improved upon in this work. The behavior of the cell during cycles can be considered for a more accurate description of the process with more in situ experiments, and its influencing factors can be explored. The present work once again shows the superiority of in situ measurements in cell research to obtain experimental data closest to the physical and chemical properties of the electrode under normal battery operating conditions. On the basis of the experimental results, to improve the cycle life of the electrodes, it is necessary to design electrodes with

CSTR: 32290.14.JUSTC-2023-0166
DOI: 10.52396/JUSTC-2023-0166
JUSTC, **2025**, 55(2): 0203

suitable pores to ensure good contact inside the electrodes while buffering the stress caused by the volume expansion of the active material.

Acknowledgements

This work was supported by the Fundamental Research Funds for the Central Universities (WK2090000055) and Anhui Provincial Natural Science Foundation of China (2308085QG231).

Conflict of interest

The authors declare that they have no conflict of interest.

Biographies

Haosong Yang is currently a master student in the Department of Thermal Science and Energy Engineering, University of Science and Technology of China, under the guidance of Prof. Peng Tan. His research mainly focuses on multi-physics coupled energy transfer and transformation in lithium-ion batteries.

Peng Tan is currently the Executive Director and Doctoral Supervisor of the Department of Thermal Science and Energy Engineering, University of Science and Technology of China. He received his Ph.D. degree from the Hong Kong Polytechnic University in 2016. His research mainly focuses on the common multi-field coupling energy transmission and transformation problems in electrochemical energy storage systems, including the exploration of multi-field coupling transmission mechanism, theoretical model construction, and regulatory mechanism research.

Lili Gong is currently an Associate Researcher at the Department of Thermal Science and Energy Engineering, University of Science and Technology of China. She received her Ph.D. degree from the Southeast University in 2021. Her research mainly focuses on lithium-ion battery technology, electric vehicles, and the interaction of power grids.

References

[1] Zhang Y, Cheng Y, Song J, et al. Functionalization-assistant ball milling towards Si/graphene anodes in high performance Li-ion batteries. *Carbon*, **2021**, *181*: 300–309.
[2] Yuan S, Duan X, Liu J, et al. Recent progress on transition metal oxides as advanced materials for energy conversion and storage. *Energy Storage Materials*, **2021**, *42*: 317–369.
[3] Yang Z, Wang T, Branch R, et al. Tidal stream energy resource characterization in the Salish Sea. *Renewable Energy*, **2021**, *172*: 188–208.
[4] Choi J W, Aurbach D. Promise and reality of post-lithium-ion batteries with high energy densities. *Nature Reviews Materials*, **2016**, *1*: 16013.
[5] Yuan S, Zhao Y, Chen W, et al. Hierarchical SnO_2 nanosheets array as ultralong-life integrated anode for lithium-ion batteries. *Nano*, **2017**, *12*: 1750077.
[6] Ma D, Yuan S, Cao Z. Three-dimensionally macroporous graphene-supported Fe_3O_4 composite as anode material for Li-ion batteries with long cycling life and ultrahigh rate capability. *Chinese Science Bulletin*, **2014**, *59*: 2017–2023.
[7] Yuan S, Zhao Y, Chen W, et al. Self-assembled 3D hierarchical porous Bi_2MoO_6 microspheres toward high capacity and ultra-long-life anode material for Li-ion batteries. *ACS Applied Materials & Interfaces*, **2017**, *9*: 21781–21790.
[8] Ohzuku T, Iwakoshi Y, Sawai K. Formation of lithium-graphite intercalation compounds in nonaqueous electrolytes and their application as a negative electrode for a lithium ion (shuttlecock) cell. *Journal of the Electrochemical Society*, **1993**, *140*: 2490–2498.
[9] Luo F, Liu B, Zheng J, et al. Review: Nano-silicon/carbon composite anode materials towards practical application for next generation Li-ion batteries. *Journal of the Electrochemical Society*, **2015**, *162*: A2509–A2528.
[10] Zhou M, Li X, Wang B, et al. High-performance silicon battery anodes enabled by engineering graphene assemblies. *Nano Letters*, **2015**, *15*: 6222–6228.
[11] Zhuang X, Zhang Y, He L, et al. Scalable synthesis of nano-Si embedded in porous C and its enhanced performance as anode of Li-ion batteries. *Electrochimica Acta*, **2017**, *249*: 166–172.
[12] Shi F, Song Z, Ross P N, et al. Failure mechanisms of single-crystal silicon electrodes in lithium-ion batteries. *Nature Communications*, **2016**, *7*: 11886.
[13] Gong X, Zheng Y, Zheng J, et al. Surface-functionalized graphite as long cycle life anode materials for lithium-ion batteries. *ChemElectroChem*, **2020**, *7*: 1465–1472.
[14] Dou F, Shi L, Chen G, et al. Silicon/carbon composite anode materials for lithium-ion batteries. *Electrochemical Energy Reviews*, **2019**, *2*: 149–198.
[15] Kim J S, Pfleging W, Kohler R, et al. Three-dimensional silicon/carbon core–shell electrode as an anode material for lithium-ion batteries. *Journal of Power Sources*, **2015**, *279*: 13–20.
[16] Li H. A high capacity nano-Si composite anode material for lithium rechargeable batteries. *Electrochemical and Solid-State Letters*, **1999**, *2*: 547.
[17] Cho J H, Xiao X, Verbrugge M W, et al. Influence of oxygen content on the structural evolution of SiO_x thin-film electrodes with subsequent lithiation/delithiation cycles. *ACS Applied Energy Materials*, **2022**, *5*: 13293–13306.
[18] Kitada K, Pecher O, Magusin P C M M, et al. Unraveling the reaction mechanisms of SiO anodes for Li-ion batteries by combining *in situ* ^{7}Li and *ex situ* ^{7}Li/^{29}Si solid-state NMR spectroscopy. *Journal of the American Chemical Society*, **2019**, *141*: 7014–7027.
[19] Nguyen C C, Choi H, Song S W. Roles of oxygen and interfacial stabilization in enhancing the cycling ability of silicon oxide anodes for rechargeable lithium batteries. *Journal of the Electrochemical Society*, **2013**, *160*: A906–A914.
[20] Lee B S, Oh S H, Choi Y J, et al. SiO-induced thermal instability and interplay between graphite and SiO in graphite/SiO composite anode. *Nature Communications*, **2023**, *14*: 150.
[21] Miyachi M, Yamamoto H, Kawai H, et al. Analysis of SiO anodes for lithium-ion batteries. *Journal of the Electrochemical Society*, **2005**, *152*: A2089.
[22] Xu Y, Yin G, Cheng X, et al. Enhanced lithium storage performance of silicon anode via fabricating into sandwich electrode. *Electrochimica Acta*, **2011**, *56*: 4403–4407.
[23] Lu W, Zhou X, Liu Y, et al. Crack-free silicon monoxide as anodes for lithium-ion batteries. *ACS Applied Materials & Interfaces*, **2020**, *12*: 57141–57145.
[24] Hardin G R, Zhang Y, Fincher C D, et al. Interfacial fracture of nanowire electrodes of lithium-ion batteries. *JOM*, **2017**, *69*: 1519–1523.
[25] Spingler F B, Friedrich S, Kücher S, et al. The effects of non-uniform mechanical compression of lithium-ion cells on local current densities and lithium plating. *Journal of the Electrochemical Society*, **2021**, *168*: 110515.
[26] Mohan S, Kim Y, Siegel J B, et al. A phenomenological model of bulk force in a Li-ion battery pack and its application to state of charge estimation. *Journal of the Electrochemical Society*, **2014**, *161*: A2222–A2231.
[27] Berckmans G, De Sutter L, Marinaro M, et al. Analysis of the effect of applying external mechanical pressure on next generation silicon

CSTR: 32290.14.JUSTC-2023-0166
DOI: 10.52396/JUSTC-2023-0166
JUSTC, **2025**, 55(2): 0203

alloy lithium-ion cells. *Electrochimica Acta*, **2019**, *306*: 387–395.
[28] Müller V, Scurtu R G, Richter K, et al. Effects of mechanical compression on the aging and the expansion behavior of Si/C-Composite NMC811 in different lithium-ion battery cell formats. *Journal of the Electrochemical Society*, **2019**, *166*: A3796–A3805.
[29] Piper D M, Yersak T A, Lee S H. Effect of compressive stress on electrochemical performance of silicon anodes. *Journal of the Electrochemical Society*, **2013**, *160*: A77–A81.
[30] Shi X, Li G, Zhang R, et al. Operation of rechargeable metal-ion batteries in low-temperature environments. *Renewable and Sustainable Energy Reviews*, **2024**, *189*: 113861.
[31] Li X, Zhang Z, Fu K, et al. Stress state characterization of Li-ion batteries based on a membrane sensor. *Energy & Fuels*, **2023**, *37*: 13526–13535.
[32] Ding L, Li D, Du F, et al. Mechanical behaviors and ion transport variation of lithium-ion battery separators under various compression conditions. *Journal of Power Sources*, **2022**, *543*: 231838.
[33] Cannarella J, Arnold C B. Stress evolution and capacity fade in constrained lithium-ion pouch cells. *Journal of Power Sources*, **2014**, *245*: 745–751.
[34] Zhu S, Yang L, Fan J, et al. *In-situ* obtained internal strain and pressure of the cylindrical Li-ion battery cell with silicon-graphite negative electrodes. *Journal of Energy Storage*, **2021**, *42*: 103049.
[35] Chen J, Yang L, Han Y, et al. An *in situ* system for simultaneous stress measurement and optical observation of silicon thin film electrodes. *Journal of Power Sources*, **2019**, *444*: 227227.
[36] Zhang J, Zhang J, Wang D, et al. Stress evolution in SiO electrodes for lithium-ion batteries during electrochemical cycling. *Materials Letters*, **2017**, *190*: 79–82.
[37] Li B, Chao Y, Li M, et al. A review of solid electrolyte interphase (SEI) and dendrite formation in lithium batteries. *Electrochemical Energy Reviews*, **2023**, *6*: 7.
[38] Tang Z, Zhou S, Huang Y, et al. Improving the initial coulombic efficiency of carbonaceous materials for Li/Na-ion batteries: Origins, solutions, and perspectives. *Electrochemical Energy Reviews*, **2023**, *6*: 8.
[39] Zhang Z, Li X, Gong L, et al. Performance of lithium-ion pouch cells with silicon composite anodes under external mechanical pressure. *Energy & Fuels*, **2023**, *37*: 9713–9721.

CSTR: 32290.14.JUSTC-2023-0166
DOI: 10.52396/JUSTC-2023-0166
JUSTC, **2025**, 55(2): 0203